Reprinted from
18 October 1974, Volume 186, pp. 207-212

SCIENCE

Computerized Transaxial X-ray Tomography of the Human Body

R. S. Ledley, G. Di Chiro, A. J. Luessenhop, H. L. Twigg

Computerized Transaxial X-ray Tomography of the Human Body

A new tomographic instrument is able to distinguish between soft tissues everywhere in the whole body.

R. S. Ledley, G. Di Chiro, A. J. Luessenhop, H. L. Twigg

The medical x-ray image may be recorded in various final forms, for example, on a fluorescent screen, on radiographic film, as a xeroradiogram, or in an electronic mode. Basically, however, the image is the result of variable transmission of the x-ray beam through tissues and body fluids that have different absorption coefficients. Medical roentgenography is at its best in the evaluation of large differential densities. These differences may be natural—bone versus soft tissue, entrapped air versus the containing cavity wall or adjacent organs—or artificial. An artificial difference can be created by the introduction of either a medium which is translucent to x-rays (such as air) or one which is opaque to x-rays (such as an iodine-containing chemical). Even at its optimal—in the presence of large differential densities—the resolution contained in the radiograph is severely limited by the fact that the shadows of the surrounding tissues overlap and are superimposed on the area under investigation.

One attempt to circumvent this difficulty resulted in the development of conventional tomography. In that technique, the radiation source (x-ray tube) moves in one direction and the recording film moves in the opposite direction; or alternatively, the patient and the film are subjected to parallel rotations. In either case, the image of one anatomical plane is kept in constant registration on the film, while the shadows of all other points of the body move and thus blur across the film. The degree of blurring, of course, increases with the distance of the point from the plane. The resultant shadowgraph is a more or less clear image of the plane under examination and nearby layers, with more distant organs blurred into (ideally) a not too distracting background. One type of tomograph, in which a slanted x-ray source rotates about an axis perpendicular to the anatomical plane, can produce images of axial-transverse (horizontal) layers of the part of the body under examination, including the brain if it is outlined by injected air (*1*). The increase in resolution obtained by tomography, although clinically useful, is not very significant.

It appeared evident to many that more efficient methods of resolving the absorption of the x-ray beam in its transmission through the various parts of the body had to be found. This led to the development of computerized axial tomography. In this system, a horizontal (transverse) layer is penetrated by a narrow x-ray beam which impinges from a large number of angles on the part of the body to be studied. The multiple transmissions are recorded by an antipodal detector so that an array of point-by-point relative absorption coefficients can be calculated.

The system of computerized axial tomography has been developed during more than a decade. Oldendorf (*2*) patented the idea of passing an x-ray beam at successive angles through an object to obtain a measure of the absorption coefficient at the rotation center. Cormack, in a remarkable paper of 1963 (*3*), discussed the idea of making measurements of the x-ray transmission "along lines parallel to a large number of different directions" so as to obtain a sequence of x-ray transmission profiles. These multiple profiles would be subjected to a Fourier type of analysis to reconstruct the linear absorption coefficients $g(r,\theta)$ in the area being scanned (r,θ are the polar coordinates). Finally, he actually carried out an experiment, using a gamma-ray source, collimating the beam to a width of 7 millimeters, and measuring the intensity of the transmitted beam at 5-mm intervals over a 12.5-centimeter scan-pass length with a Geiger-Müller counter. An aluminum cylinder surrounded by a wooden annular ring was scanned and the absorption coefficients were calculated; the experimental results agreed with the actual absorption coefficients of the materials within one to two significant figures. Cormack noted that his results were applicable to the field of radiology, for "the determination of a variable x-ray absorption coefficient in two dimensions." Thus, the essence of computerized axial tomography is already contained in Cormack's contribution, which represents a specific application of the more general methodology of image reconstruction. This methodology may be used in fields as diverse as astronomy and electron microscopy. A bibliography of the mathematical reconstruction methods has been compiled by Gordon (*4*).

The first commercial instrument capable of obtaining high-resolution images useful for medical purposes was designed by Hounsfield. This British investigator introduced the EMI-Scanner (*5*), with which information re-

Dr. Ledley is president of the National Biomedical Research Foundation and professor of physiology, biophysics, and radiology at Georgetown University, Washington, D.C. 20007. Dr. Di Chiro is head of the section on neuroradiology, National Institutes of Health, Bethesda, Maryland 20014, and clinical professor of radiology, Georgetown University. Dr. Luessenhop is chief of neurological surgery, Georgetown University. Dr. Twigg is chairman of radiology, Georgetown University.

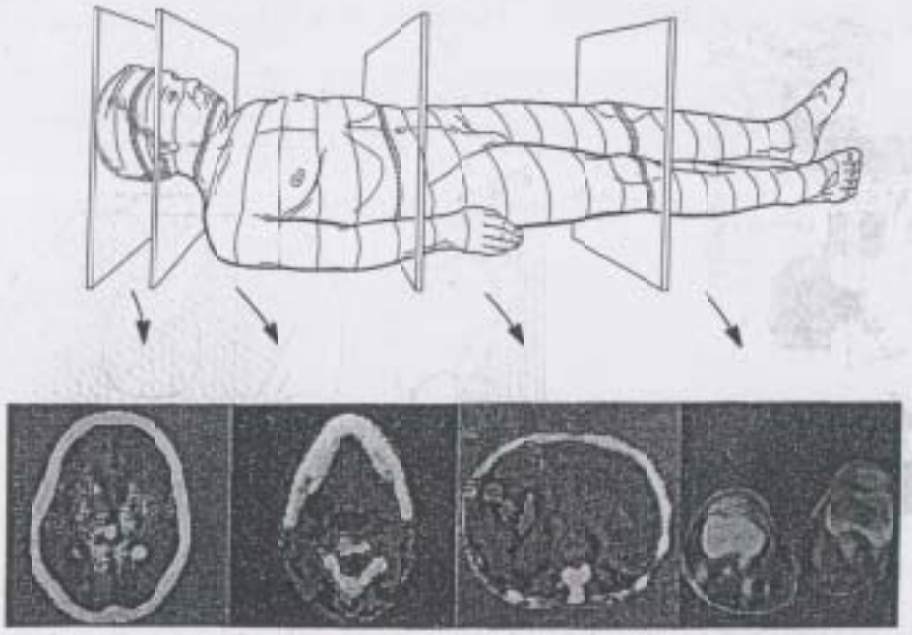

Fig. 1. Capability of ACTA-Scanner for evaluating every part of the body. The striations represent typical cross sections that can be made, with four specific illustrations.

garding the soft tissues in the head, particularly the brain and the endocranial cerebrospinal-fluid cavities, can be gathered. No parts of the body other than the head can be examined with the EMI-Scanner, because the device cannot handle large differences in the absorption coefficients of contiguous areas. The necessity of interposing an absorption-equilibrating medium, such as water, makes it impractical to study sections of the body other than the head. In addition, parts of the body such as the chest and abdomen could not be evaluated by a system similar to the EMI-Scanner, even if the outside absorption-equilibrating medium was used, because of their internal gaseous content. The instrument described below does not need a water intermediary.

ACTA-Scanner

The new x-ray scanner described here, called the Automatic Computerized Transverse Axial Scanner (ACTA-Scanner) (*6*), has the great advantage that it is capable of evaluating every part of the body (see Fig. 1). With the ACTA-Scanner, as the highly collimated x-ray beam traverses the body, some photons are absorbed, while others pass through and are detected by a sodium iodide crystal. The absorption along any path depends on the sum of the absorption coefficients of the tissues through which the beam passes. A flash of visible light is emitted for each x-ray photon impinging on the crystal, and a photomultiplier observing the light output of the crystal samples the transmitted beam intensity as the integrated current that is produced in 5-millisecond intervals. The x-ray intensity profile made during a single scan-pass consists of 160 such measurements. The translation carriage is then slightly rotated and another scan-pass is made, producing another profile, and so forth. A completed scan can be composed of up to 180 scan-passes, with the carriage being rotated 1° for each pass (Fig. 2).

To see why the results are so accurate, note that every point in the cross section is scanned during each scan-pass. Thus, after 180 scan-passes, each point has been "measured" 180 times. The 180 x-ray profiles of the section are then processed by the computer, which reconstructs the tissue absorption coefficient at each point, forming the array of picture points. Up to 25,600 points are reconstructed, forming a raster of 160 by 160 points. Compare this with a plain x-ray image, in which all the points along the beam's path overlap, and with a conventional tomographic picture, in which the plane being observed is overlaid with blurred images of the tissues over and under it.

In the head, clear images of the cerebral ventricles and the larger subarachnoidal cavities (interhemispheric and sylvian fissures) are obtained. The eyeballs stand out in the orbits, and the facial sinuses, which contain air, are strikingly visualized. The various soft tissues and formations of the cervical area, including not easily accessible structures such as the spinal cord, are depicted. In the chest, the lungs, heart, and mediastinal structures are evident, and in the abdomen and pelvic region the various viscera are displayed; not only the outlines but also the details of their inner structure are shown. In the limbs, the muscles, neurovascular bundles and fine ligamentous-cartilaginous elements of the joints are shown.

The algorithm for reconstructing a two-dimensional picture section from a sequence of one-dimensional x-ray profiles is based on a theorem from two-dimensional Fourier analysis. This theorem states that the Fourier transform of a one-dimensional projection of an object is identical to the corresponding central section of the two-dimensional Fourier transform of the object. That is, the Fourier transform of the x-ray profile from a scan-pass at a given angle is identical to the value of the Fourier transform of the two-dimensional section in the plane of the scan-pass along a line through the center of the transform at the same angle. At the end of a complete scan, 180 transform images have been accumulated, each of which corresponds to the proper central transform image of the original cross section. The inverse transform of this complete transform image is the reconstructed cross section.

In particular if $p(l,\theta)$ is the profile taken at an angle θ, where l is the distance along the scan-pass, then the Fourier transform relations are

$$p(R,\theta) = \int_{-\infty}^{+\infty} p(l,\theta) e^{-i2\pi Rl}\, dl$$

$$g(r,\phi) = \int_{0}^{2\pi} \int_{0}^{+\infty} p(R,\theta) e^{-i2\pi R r \cos(\theta-\phi)} R\, dR\, d\theta$$

where R is the distance along the line in the transform space; r,ϕ are polar coordinates for the reconstructed picture; and $g(r,\phi)$ are the relative absorption coefficients. A real-time programming approach was adopted with the ACTA-Scanner, so that the reconstructed picture is available as soon as a complete scan is finished.

It is difficult to formulate the precise physical interpretation of the "relative absorption coefficients" that comprise the points of the picture matrix. This is because the bremsstrahlung, or continuous x-ray spectrum, is the major

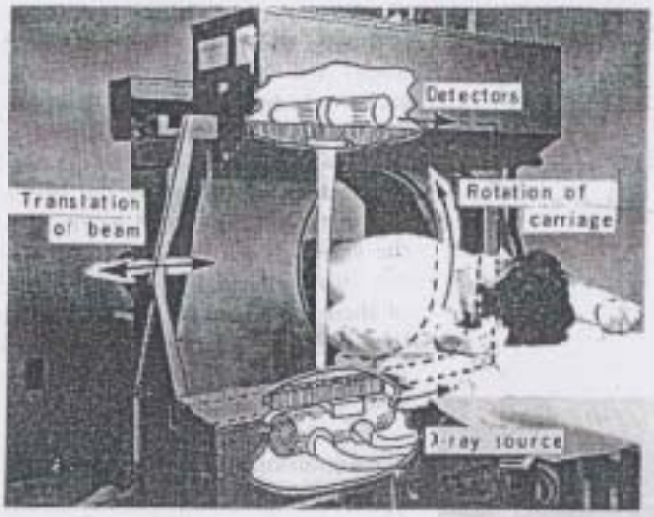

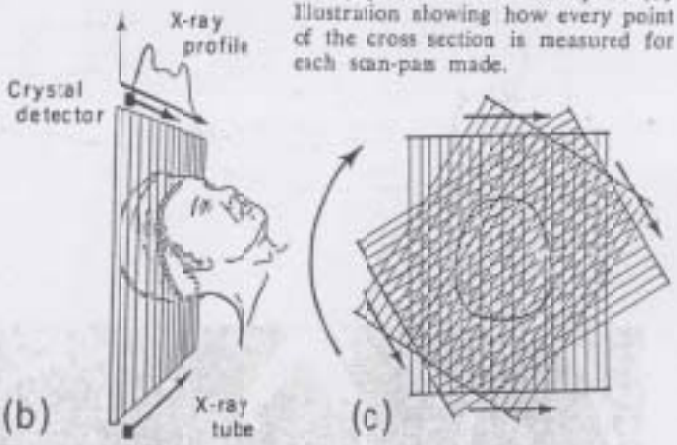

Fig. 2. (a) Diagram of the ACTA-Scanner showing the translation carriage and rotation assembly. (b) Illustration of intensity profile for one scan-pass. (c) Illustration showing how every point of the cross section is measured for each scan-pass made.

component of the x-ray beam emitted by the tungsten target. The value of the mass-absorption coefficient for x-rays through any material is dependent on x-ray frequency and on the "concentration of Z," that is, on the atomic numbers (Z) and density of the absorbing material in the path of the beam.

For organic substances, such as muscle, blood, and tendons, specific gravity may be the most useful variable to correlate with our relative absorption coefficient. This is because these materials have about the same proportion of carbon, nitrogen, oxygen, and hydrogen, and therefore the main distinguishing feature among them is their respective densities. Of course, this rule does not hold for special substances, such as bone with its high calcium content, or when various solutions containing iodine or other elements of high atomic number have been injected into body systems to enhance the contrast of the x-ray image. Hence, some care must be used in the interpretation of the relative absorption coefficient values produced by the ACTA. Clinical evaluation, however, has indicated that these numbers can be interpreted in compositional terms. Thus, in an oleothorax (see third row of Fig. 3), oil injected into the chest can be seen in a cystic cavity contrasting with the denser body fluids and with the even more dense fibrous tissue of the cyst wall. In tumoral masses, the absorption coefficients permit the classification of lesions as softer or harder than the normal surrounding tissues; the correlation of the degree of softness or hardness with specific histologic tumoral types represents a challenging prospect.

However, even this specific gravity rule of thumb must be used with caution. With the ACTA-Scanner it has been observed that the relative absorption coefficient for low Z biological materials actually correlates with the electron density of the material, rather than with the mass density (*7*). This result is consistent with x-ray absorption theory. The importance of this observation can be seen, for example, in the case of blood: a calculation shows that the difference between the electron density of a blood clot and that of whole blood is not as large as the difference between the mass densities, and therefore the ACTA-Scanner coefficients will not reflect the larger mass-density difference.

ACTA Display for Clinical Use

In the design of the ACTA display, methods of pattern recognition (*6*) were used to facilitate clinical analysis of the pictures. The display units are a 19-inch color television set and two 12-inch black-and-white television sets, one of which is used for photography and the other for viewing. One complete scan produces two pictures of adjacent cross sections, each 7.5 mm thick, with a 3-mm space between them. Both pictures appear on the television screens immediately after the scan is completed. To examine the brain, for example, about three or four scans are made, producing six to eight cross-section pictures. The pictures can be photographed and stored on digital magnetic tape or cassettes.

The description of the features of the display is simplified by first defining certain terms. The computer reconstructs a relative absorption coefficient for each element in the picture corresponding to a block, or volume of body tissue, with edges 1.5 by 1.5 mm in the plane of the section, and 7.5 mm thick. Each picture is composed of an array of 160×160 ($=25{,}600$) such picture elements, called pictels. Thus, each pictel has an associated numerical value, called the ACTA number, which is the relative absorption coefficient of the corresponding tissue block of the body section. By the time the scan is completed the ACTA numbers of all the pictels have been computed and are stored as numbers in the computer's memory. The values of the ACTA numbers that can be displayed are from 0 to 2048. For any particular picture, the operator can choose to display only a limited range of ACTA numbers, as specified by a mean and window width. Thus, if the operator specifies a mean of 206 and a width of 14, as in the first row of Fig. 3, then the range of numbers that will be displayed is from 200 to 213, inclusive, or if a mean of 260 and width of 100 are specified, as in the third row of Fig. 3, then the range of numbers displayed will be from 111 through 410. How these numbers are actualy "seen" in the picture is described as follows.

The ACTA display television tubes are capable of showing 16 different colors (or gray levels) at a time. A color-coded key is used to visually relate to pictel values. In the display of the picture, each of these 16 different colors (or gray levels) represents a specific range of ACTA numbers. The correspondence of colors (or gray levels) to number ranges is shown in the heading of the display, for easy reference. In the heading, 16 boxes labeled by box numbers 0 through 9 and A

spectivey. Computer programs have been written to allow the user to enter the mean and window width, and also to assign the number ranges in unequal intervals, if desired.

The color spectrum for the color-coded key can be chosen by the user. A continuous spectrum, as in the first row of Fig. 3, or a contrasting spectrum, as in the third row of Fig. 3, can be used. A contrasting spectrum can often be used to clearly distinguish structures, as in the picture through the orbits of the first row of Fig. 3.

A number of computer programs are available to assist the clinician in the analysis of the picture. For example, programs are available to blacken all picture elements with values in the range of a given color box. This capability facilitates the accurate determination of the coefficient value for each element of the picture. It can be used to accentuate features of particular coefficient values. Judicious choice of the blackened color boxes can frequently be used to outline various structures. Additional programs can obtain the area covered by the elements blackened, and can "flicker" the blackened boxes to make them more easily discernible to the eye.

Other Aspects

The ACTA has great mechanical versatility. Since it can be used to scan anywhere on the whole body, it has both a long scan-pass of 48 cm and a short scan-pass of 24 cm. The short scan-pass is used for the head, neck, and extremities, and the long one for the thorax, abdomen, and pelvis. A complete 180° scan takes less than 5 minutes with the short scan-pass and about 6 minutes with the long scan-pass. In addition the plane of the scan can be tilted in a 30° arc in order to produce exactly the proper cross section for the clinical problem at hand.

The x-ray voltage used varies from 90 to 120 kilovolts, with anode currents of 10 to 15 milliamperes, depending on the case. The maximum x-ray exposure to the skin is about 1 rad for a complete scan, the rad being a measure of dose per unit volume. This is about equal to the maximum dose received in a single conventional skull x-ray, except that in ordinary x-ray imaging the entire head receives the x-ray dose. Thus, since a rad is dose per unit volume of tissue, and since only the sections being scanned are irradiated, the total dose received by the patient for a series of three or four ACTA scans covering the head is about the same as the total dose received by the patient for a single head x-ray. The scatter from the ACTA is extremely small, because the x-ray beam is well collimated. During operation, the scatter is primarily from the patient.

Some motion of the patient while the scan is being made can be tolerated. In particular, an excursion of short duration will not interfere with the picture, provided that the body part returns to its original position. Periodic motions, such as those involved in breathing or the heart beat, will result in some type of averaged result dependent on the proportion of time the oscillating part spends in each location during the scan.

Preliminary Clinical Results

Figure 3, first row, shows the very first ACTA-gram, or picture made by the ACTA; this is a cross section of a navel orange placed inside a human skull, all of which was placed in water in a bowl. Our clinical experience in the last 4 months, since the ACTA-Scanner was first used on patients, has

Fig. 3. ACTA-grams. (First row, left) The first picture made by the ACTA-Scanner. A navel orange was placed inside a human skull (of the type used by medical students, where the skull "cap" can be removed for studying inside the cranium and reattached with clips), and the skull was placed in a plastic bowl of water; the water easily flows into the skull through the various fissures and foramina, and the orange floats in the water. The ACTA-gram is of a vertical cross section of the bowl; note that the less dense "white" part of the orange peel is clearly visible, and above the water level the more dense "orange" part of the peel can be distinguished. (First row, middle) Sections of the brain (with continuous color spectrum). The tomographic layer on the right at the level of the foramen of Monro displays the frontal horns of the lateral ventricles separated by the septum pellucidum, the third ventricle, and the calcified pineal body and choroid plexuses; the latter are located within the trigona of the lateral ventricles, which are also clearly demonstrated. Also evident are the interhemispheric fissure in front and the increased bilateral paraventricular densities, probably corresponding to the basal ganglion. The section on the left is higher, showing more of the ventricles. (First row, right) Illustration of the effectiveness of using contrasting colors in distinguishing various tissues by their characteristic densities: a section is shown through the eyes, the middle cranial fossae, and the posterior cranial fossa. The right ocular bulb is clearly defined (green), with its retro-orbital fat posteriorly and lacrimal gland anteriorly (both reddish brown); the optic nerve is seen coursing back to the brain. The right middle fossa is larger than the left and its tissue is less dense because of a tumor (astrocytoma); in the posterior fossa, the cerebellar hemispheres can be distinguished posterior to the petrous portion of the temporal bone, while laterally the mastoid sinuses appear. Outside the skull can be seen structures of the neck posteriorly and the temporal muscle (brown) laterally. (Second row, left to right) Enlarged ventricles with calcified choroid plexuses. Craniopharyngioma; arrows point to cystic cavity, with solid mass in center. Cerebral hematoma (clotted blood is yellow and grey). Mandible and a cervical vertebra: note the mandibular canals (blue) and structures around and within spinal canal. (Third row, left) The section at the right shows a tumoral nodule in the left lung as viewed from below; a contrasting color spectrum is used. Note the mediastinal structures (trachea, black; aortic arch and vena cava, light blue) and bones (sternum, vertebra, ribs, and scapulas; white); the section on the right is higher than that on the left and shows less of the aortic arch. (Third row, middle) Chest layer through the anterior fifth rib, in a patient with left oleothorax: many years previously some type of oil had been injected into the patient's lung, probably as a treatment for tuberculosis, and a fibrous capsule formed which now encloses both the oil and some serous fluid. The ACTA-gram was made with the patient lying on his back, and the horizontal fluid interface between the oil (green) floating on top of the watery serous fluids (tan) is clearly seen. The heart image appears in front: the outline of its various chambers, as seen at this particular level, and the different density gradients of the heart cavities can be seen. The normal right lung and the left lung, compressed by the posterolateral lesion, are clearly seen, as are the pulmonary vessels entering the lungs. The spine with its central canal and the aorta on the left of the spine are also seen. (Third row, right) Same oleothorax displayed with a narrower window to show the lesion in more detail; the color scale shows increasing density from left to right. Note the fluid levels, corresponding to oil (brown), emulsified mixture (light tan), and body fluids (dark green). The fibrous capsule (light green) has the same density as heart muscle. (Fourth row, left to right) Section through knees showing details of bony structures, including marrow of patellas, and cancellous bone of femur condyles. Scan through knees showing patellas, femurs, and (posteriorly) tendons. Medial meniscus seen in right knee. Color rendition of medial meniscus: color just below bone density is blackened, outlining right tibial protuberance (white); color just below cartilage density is blackened, outlining meniscus (yellow).

through F (the letters representing 10 through 15) are pictured, each box containing its ACTA number range on a background of the corresponding color (or gray level), as shown in Fig. 3.

Thus, in a picture display, the color (or gray level) of each of the 25,600 pictels represents its corresponding ACTA number value according to the heading. For a typical picture display, the color of box 0 represents all the points of value less than the range, and the color of box F represents all the points of value greater than the range. The numbers within the range are equally distributed among the 14 remaining colors. Thus, for a window width of 14 and a mean of 206, as shown in the first row of Fig. 3, the color boxes 1, 2, 3, . . . , E represent the ACTA numbers 200, 201, 202, . . . , 213, respectively; the boxes 0 and F represent ranges 0–199 and 214–2047, respectively. Or for a width of 300 and mean of 260, as shown in the third row of Fig. 3, the color boxes 1, 2, 3, . . . , E represent, respectively, the number ranges 111–131, 132–152, 153-174, . . . , 388–409; boxes 0 and F represent ranges 0–110 and 410–2047, re-

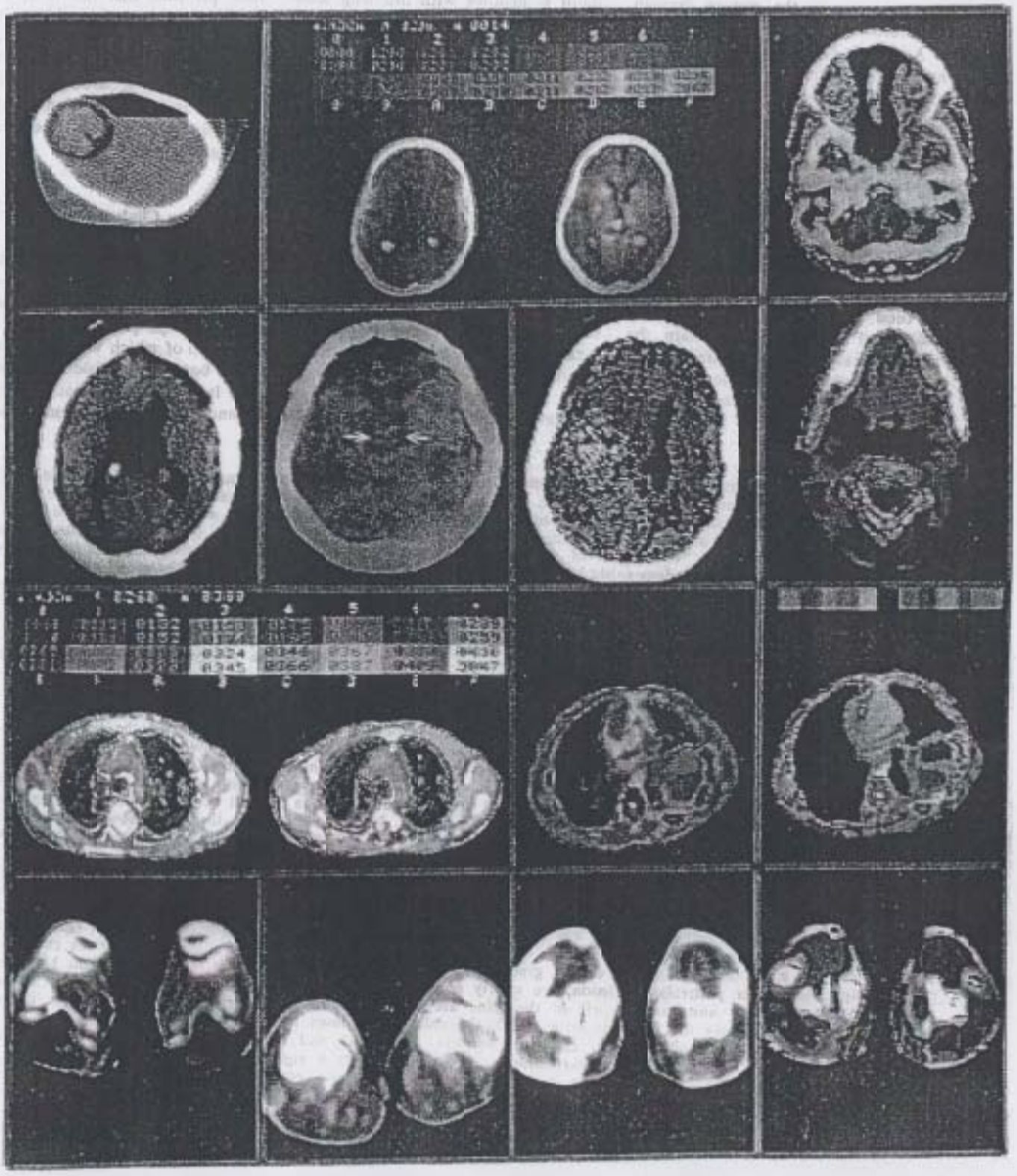

confirmed that this device allows us to study every part of the human body. However, most of the approximately 400 patients we have studied have been examined because of clinical suspicion of endocranial pathology. Thus, we have obtained clear images of the lateral ventricles and third ventricle (for example, see first row of Fig. 3). The fourth ventricle and some of the larger subarachnoidal cavities (interhemispheric and sylvian fissures) are also seen. Often, the brainstem is well outlined. Occasionally, we have been able to recognize areas of increased density in the region of the basal ganglia, which may correspond to the deep gray-matter nuclei. Of course, whenever structures containing physiologically high calcium levels (such as calcified pineal or choroid plexuses) are present, these will stand out quite strikingly (Fig. 3). The evaluation of the orbits, the posterior fossa, and the base of the skull is very rewarding (Fig. 3, first row). Such pathological conditions as hydrocephalus (Fig. 3, second row) and tumors (Fig. 3, second row) have been demonstrated. A particularly high degree of reliability has been encountered in visualizing intracerebral bleeding (Fig. 3, second row).

In the study of parts of the body other than the skull and the brain, the ACTA-Scanner has unique capabilities. We have already obtained useful diagnostic information in the evaluation of the craniocervical junction, the cervical spine, the hindbrain, the cervical spinal cord, the chest, the abdomen, the pelvis, and the upper and lower limbs. Because of the inherent problem of the motion of the intrathoracic organs, and considering the time required for each scan (between 5 and 6 minutes), we had some doubts about the usefulness of the scanner in evaluation of the chest. However, we have been favorably surprised by the detail demonstrable in these ACTA-grams (Fig. 3, third row). Thus, lungs, heart, mediastinal structures, and thoracic spine are clearly visualized. In the abdomen and pelvis, one recognizes the large viscera and some of their inner structure. In the limbs, besides the bony elements, one may also delineate muscles, vasculoneural bundles, and fine cartilaginous components of the joints (Fig. 3, fourth row).

Conclusions

The ACTA-Scanner has virtually unlimited potential in the evaluation of any part of the body. The usefulness of the technique has already been shown in the appraisal of pathologies of the brain and cerebrospinal fluid cavities. The orbits and the eyeballs, the facial sinuses, and skull base lesions have also been elucidated.

Tumors of the larynx, pharynx, thyroid, and parathyroid; lymphomas; and pathology of the spine and spinal cord are well within the reach of this new diagnostic methodology. Lung pathologies, such as emphysema, pneumonias, neoplasms, infarctions, pleural effusions and granulomatous diseases, and mediastinal pathology represent a challenging complex of lesions to be appraised by ACTA-scanning. For the heart, there is great potential for observing cardiac chamber size, hypertrophy of ventricular or atrial walls, and ventricular or aortic aneurysms, and possibly for recognizing the damaged myocardial tissue immediately after or some time after an infarction. The abdominal pathologies that can be studied are almost uncountable: gastric neoplasms, pancreatic cysts and stones, gallstones, neoplasms of the liver and pancreas, bowel tumors, abdominal aortic aneurysms, renal neoplasms and cysts, atrophy of the kidneys, bladder tumors, uterine tumors, ovarian cysts, and many more. Although bones and joints are adequately demonstrated by conventional x-ray techniques, there is no doubt that as the new technique is developed ACTA-grams will contribute significant information in the transverse plane, as well as in densitometric analyses.

The impact of ACTA-scanning will not be limited to the diagnostic area, but will extend, at least indirectly, to general patient management and to some aspects of medical economics as well. Risk-laden, technically complex, and costly diagnostic procedures, sometimes requiring lengthy hospitalization, will in some cases be eliminated. The simple, innocuous, and noninvasive ACTA-scanning can be performed on an outpatient basis. Repeated follow-up examinations should be easily accepted by the patients, considering that this diagnostic test is carried out without discomfort. The entire field of diagnostic radiology is on the verge of revolutionary changes.

References and Notes

1. G. Di Chiro, *Am. J. Roentgenol. Radium Ther. Nucl. Med.* **92**, 7 (1964).
2. W. H. Oldendorf, *IRE (Inst. Radio Eng.) Trans. Bio-Med. Electron.* **8** (No. 1), 68 (1961).
3. A. M. Cormack, *J. Appl. Phys.* **34**, 2722 (1963).
4. R. Gordon, "A bibliography on reconstruction from projections," Mathematical Research Branch, National Institute of Arthritis, Metabolism, and Digestive Diseases, Bethesda, Maryland (1973).
5. References on the EMI-Scanner: G. N. Hounsfield (part 1) and J. Ambrose (part 2), *Br. J. Radiol.* **46**, 1016 (1973); H. L. Baker, J. K. Campbell, O. W. Houser, D. T. Rose, P. F. Sheedy, C. B. Holman, R. L. Kurland, *Mayo Clin. Proc.* **49**, 17 (1974); P. F. J. New, W. R. Scott, J. A. Schnur, K. R. Davis, J. M. Taveras, *Radiology* **110**, 109 (1974).
6. See, for example, R. S. Ledley, in *AFIPS (Am. Fed. Inf. Process. Soc.) Conf. Proc.* **42**, 461, 481 (1973); R. S. Ledley, H. A. Lubs, F. H. Ruddle, *Comput. Biol. Med.* **2**, 108 (1972); R. S. Ledley, *IEEE (Inst. Electr. Electron. Eng.) Trans.* **57**, 2017 (1969).
7. W. E. Kiker, T. W. Hinz, R. S. Ledley, in preparation.
8. The ACTA-Scanner was designed by R. S. Ledley and built by the National Biomedical Research Foundation, with J. B. Wilson in charge of software, T. Golab in charge of electronics and L. S. Rotolo as industrial coordinator. Patents are pending in the name of R. S. Ledley. The clinical staff includes E. Schellinger and S. Axelbaum. We also greatly appreciate the encouragement of many colleagues at the Georgetown University Medical Center, including H. J. Curl, J. Haubert, C. Himmelsbach, L. Lilienfeld, M. McNulty, D. O'Doherty, C. Rath, J. Rose, and J. Stapleton.

160 × 160

120 kV 16 mA